ABOUT KINEMATIC ANALYSIS AND SYNTHESIS OF 3-CARDAN TRANSMISSION

Săulescu Radu, Borca Alina, Crețescu Nadia,

Universitatea Transilvania din Braşov, B^{dul} Eroilor Nr. 29, 2200, Braşov

Abstract: *The base relations that describe the generalized kinematical model of a n-Cardan transmission are proposed in the first part of this paper. On the basis of this model, in the paper is exemplified the 3-Cardan transmission synthesis by knowing the angles generated by the projections of cardanic shafts on 2 rectangular plans.*

Key words: *n-Cardan transmissions, 3-Cardan transmissions, constructive modeling, analyze and synthesis*

1. INTRODUCTION

For the cinematic modeling of a n-Cardan transmission, there are considered two successive joints *i* and *j* (Fig. 1 and 2); the following three steps are crossed: **1°** To establish the angles $(\theta x)_{ij}$, $(\theta y)_{ij}$, $(\theta z)_{ij}$ expressions depending on the angles α_i and ν_{ij}; with $(\theta x,y,z)_{ij}$ are noted the angles which are formed by the Cardan shafts versors with trihedral axes *Oxyz* (see Fig. 3), which define the projection plane (see Fig. 2); **2°** To establish the correlation's between the angles δ_{ij}, γ_{ij} and the angles $(\theta x)_{ij}$, $(\theta y)_{ij}$, $(\theta z)_{ij}$ (see Fig. 3); **3°** To determine the angles α_i and ν_{ij} depending on the angles δ_{ij} şi γ_{ij} (see Fig. 1 and 2).

In Fig. 3, $\overline{OM}$ is the associate versor of a Cardan shaft; based on this figure, are deduced the following correlation's between the angles θx, θy, θz, which become $(\theta x)_{ij}$, $(\theta y)_{ij}$, $(\theta z)_{ij}$ after generalization, and the angles δ, γ, which become δ_{ij}, γ_{ij} after generalization:

$$\operatorname{tg}\delta_{ij} = \frac{c(\theta y)_{ij}}{s(\theta x)_{ij}}, \ \operatorname{tg}\gamma_{ij} = \frac{c(\theta z)_{ij}}{c(\theta x)_{ij}}. \tag{1}$$

and reciprocal (see fig. 3):

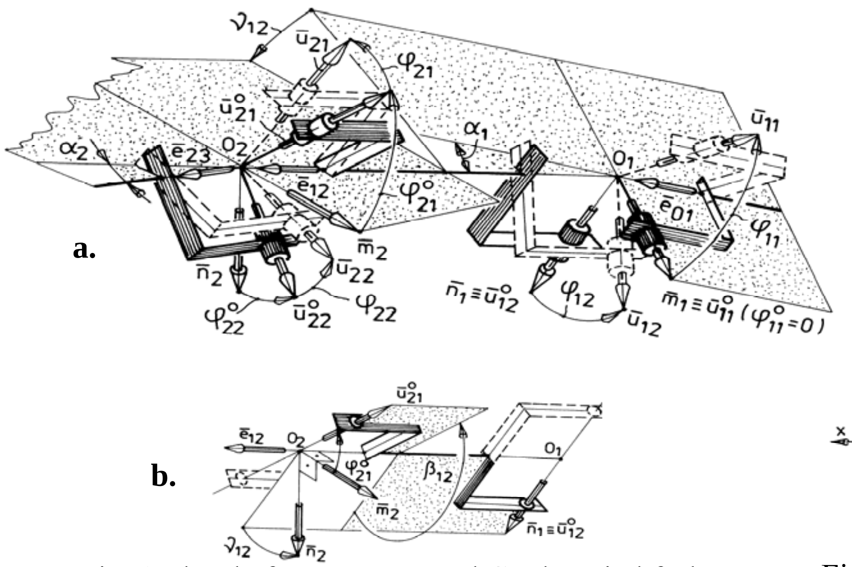

Fig. 1 The shafts geometry and Cardan pitchfork.

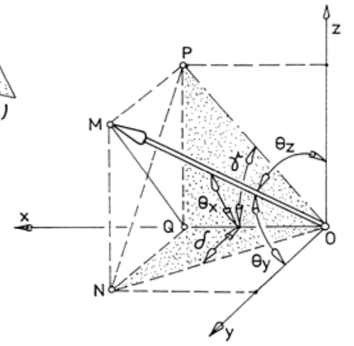

Fig. 3 The versor angle $\overline{OM}$

$$\operatorname{tg}\theta x = \sqrt{\operatorname{tg}^2\delta + \operatorname{tg}^2\gamma} \Rightarrow c\theta x = {}^{1}\!/\!\sqrt{\ },\quad c(\theta x)_{ij} = {}^{1}\!/\!\sqrt{\ },\ c(\theta y)_{ij} = {}^{\operatorname{tg}\delta_{ij}}\!/\!\sqrt{\ },\ c(\theta z)_{ij} = {}^{\operatorname{tg}\gamma_{ij}}\!/\!\sqrt{\ } \tag{2}$$

$$c\theta y = c\theta x \operatorname{tg}\delta,\ c\theta z = c\theta x \operatorname{tg}\gamma$$

where: $\sqrt{\ } = \sqrt{1 + \operatorname{tg}^2\delta + \operatorname{tg}^2\gamma} = \sqrt{1 + \operatorname{tg}^2\delta_{ij} + \operatorname{tg}^2\gamma_{ij}}\,, c = \cos, s = \sin$

In Fig. 2, a and b are represented two successive Cardan joints O_i and O_j, from a n-Cardan transmission; adjoining, in Fig. 2, c and d are represented the Cardan shafts projections in two rectangular planes: *xz* and *xy*. Based on Fig. 2 and relation (2), are deduced the following general correlation, where $h = i - 1,\ j = i + 1, k = j + 1$:

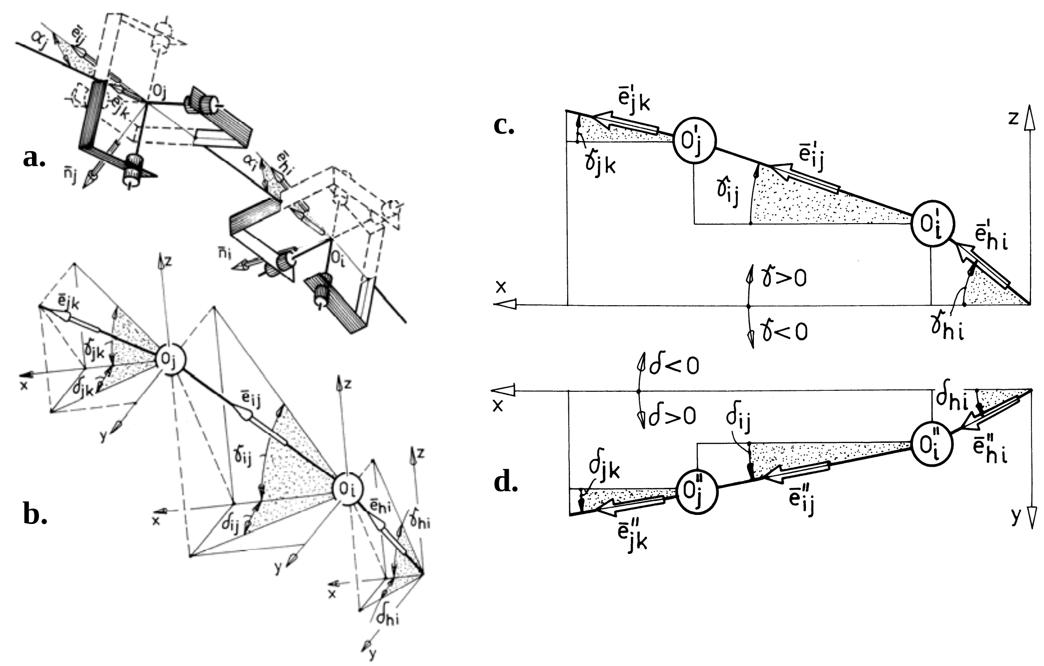

Fig. 2 The Cardan shafts projections.

$$c\alpha_i = \frac{1+\operatorname{tg}\delta_{hi}\operatorname{tg}\delta_{ij}+\operatorname{tg}\gamma_{hi}\operatorname{tg}\gamma_{ij}}{\sqrt{\left(1+\operatorname{tg}^2\delta_{hi}+\operatorname{tg}^2\gamma_{hi}\right)\left(1+\operatorname{tg}^2\delta_{ij}+\operatorname{tg}^2\gamma_{ij}\right)}}, \tag{3}$$

$$c\nu_{ij} = \frac{c\alpha_j c\alpha_i - c(\theta x)_{hi}\, c(\theta x)_{jk}\left(1+\operatorname{tg}\delta_{hi}\operatorname{tg}\delta_{jk}+\operatorname{tg}\gamma_{hi}\operatorname{tg}\gamma_{jk}\right)}{s\alpha_i s\alpha_j} \tag{4}$$

$$\begin{aligned} s\nu_{ij} = \frac{c(\theta x)_{hi}\, c(\theta x)_{ij}\, c(\theta x)_{jk}}{s\alpha_i s\alpha_j}\Big(&\operatorname{tg}\gamma_{hi}\operatorname{tg}\delta_{jk}+\operatorname{tg}\gamma_{ij}\operatorname{tg}\delta_{hi}+ \\ &+\operatorname{tg}\gamma_{jk}\operatorname{tg}\delta_{ij}-\operatorname{tg}\delta_{hi}\operatorname{tg}\gamma_{jk}-\operatorname{tg}\delta_{ij}\operatorname{tg}\gamma_{hi}-\operatorname{tg}\delta_{jk}\operatorname{tg}\gamma_{ij}\Big). \end{aligned} \tag{5}$$

Taking into account relations (4) and (5), the angle ν_{ij} can be calculate with one of the two following relations:

$$\nu_{ij} = \operatorname{sgn}(s\nu_{ij})\cdot arcc(c\nu_{ij}),\ \nu_{ij} = 2\operatorname{arctg}\frac{s\nu_{ij}}{1+c\nu_{ij}}. \tag{6) (7}$$

Relations (6) and (7) allow avoiding, on computer, the calculus and interpretation of main indeterminations.

In the case of a transmission with three Cardan gears, the cinematic model is described by the relations (1) …(7), which after simplification can be write as follows:

$$\begin{cases}\alpha_1 = \alpha_1(\delta_{01},\gamma_{01};\delta_{12},\gamma_{12}),\\ \alpha_2 = \alpha_2(\delta_{12},\gamma_{12};\delta_{23},\gamma_{23}),\\ \alpha_3 = \alpha_3(\delta_{23},\gamma_{23};\delta_{34},\gamma_{34});\end{cases} \qquad \begin{cases}\nu_{12} = \nu_{12}(\delta_{01},\gamma_{01};\delta_{12},\gamma_{12};\delta_{23},\gamma_{23};\alpha_1,\alpha_2),\\ \nu_{23} = \nu_{12}(\delta_{12},\gamma_{12};\delta_{23},\gamma_{23};\delta_{34},\gamma_{34};\alpha_2,\alpha_3),\end{cases}$$

$$\begin{cases}\beta_{12} = \nu_{12}+90^\circ+\varphi_{21}^0-\operatorname{arctg}\dfrac{\operatorname{tg}\varphi_{11}^0}{c\alpha_1},\\ \\ \beta_{23} = \nu_{23}+90^\circ+\varphi_{31}^0-\operatorname{arctg}\dfrac{\operatorname{tg}\varphi_{21}^0}{c\alpha_2};\end{cases} \qquad \begin{cases}\varphi_{11}^0 = 0^\circ\\ \varphi_{21}^0 = f_1(\alpha_1,\alpha_2,\alpha_3),\\ \varphi_{23}^0 = f_2(\alpha_1,\alpha_2,\alpha_3),\end{cases} \tag{8}$$

The obtained *generalized cinematic model* is applied for *analysis* and *synthesis* of the *homokinetic* 3-Cardan transmissions.

In Fig. 4,a, b, there are given the configurations of two 3-Cardan transmissions, through their projections in two rectangular planes, without the frontal views of intermediate shafts.

Based on the angles (δ_{ij}, γ_{ij}) described by the Cardan shafts projections (Fig. 4,a,b) it is asked to analyze if these transmissions can be homokinetic (analysis problem) and, if there are, to be determined the angles β_{12} and β_{23} values (see Fig. 4, c and d) for which the transmission are homokinetical (particular problem of synthesis).

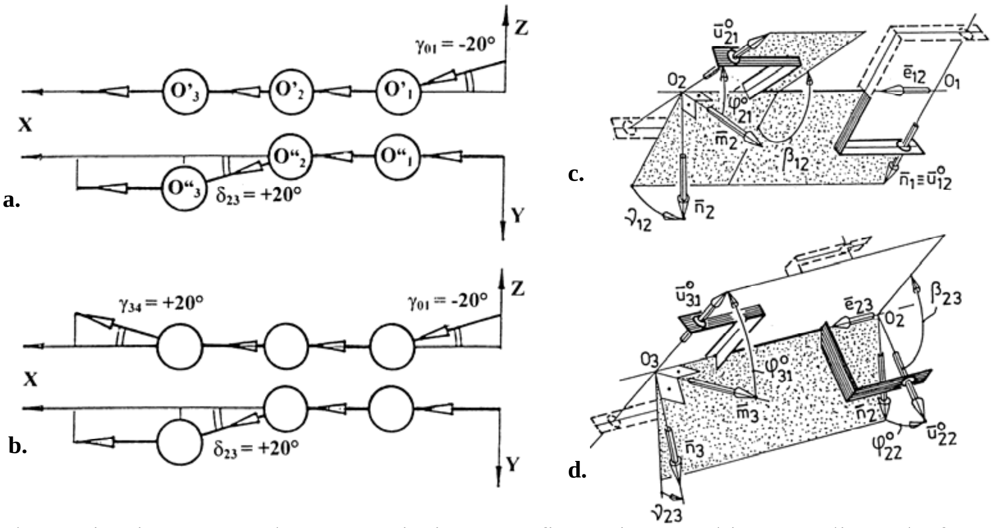

Fig.4 The projections 3-Cardan transmissions configurations and intermediary shafts geometry.

2. SOLUTION

The angles (δ_{ij}, γ_{ij}) being known, the solution will use the cinematic modeling of the homokinematic conditions, in a general form (8). Based on relations (8) and on the angles (δ_{ij}, γ_{ij}) from Fig. 4,a and b, there are determined the parameters α_1, α_2, α_3 and ν_{12}, ν_{23}; if the obtained values of the angles α_1, α_2 and α_3 satisfy the compatibility conditions (9), it means that the considering transmissions have at least one homokinetic solution.

$$\cos\alpha_1 \geq \cos\alpha_2 \cdot \cos\alpha_3, \cos\alpha_2 \geq \cos\alpha_3 \cdot \cos\alpha_1, \cos\alpha_3 \geq \cos\alpha_1 \cdot \cos\alpha_2 \quad (9)$$

In order to establish these solution, first, there are determined the angles φ_{21}^0 and φ_{31}^0 from the relations (8) and based on them there are calculated the angles β_{12} and β_{23}. After running the program based on the relations' (8) and (9), on computer there are obtained the numeric values systematized in Table 1.

	Fig. 4 a, c, d	Fig. 4 b, c, d						
Given measures								
δ_{01}	0°	0°	*Calculating measures*					
γ_{01}	– 20°	– 20°	α_1	20°	20°	ν_{12}	– 90°	– 90°
δ_{12}	0°	0°	α_2	20°	20°	ν_{23}	180°	+133,22
γ_{12}	0°	0°	α_3	20°	27,991	β_{12}	+ 60°	0°
δ_{23}	+20°	+20°	φ°_{11}	0°	0°	β_{12}*	– 60°	0°
γ_{23}	0°	0°	φ°_{21}	± 60°	0°	β_{23}	+150°	+133,22
δ_{34}	0°	0°	φ°_{31}	758,45	790°	β_{23}*	+29,97°	+313,22
γ_{34}	0°	+20°						

Table 1 Input dates and calculating for 3-Cardan transmission

The obtained values from Table 1 for the angles α_1, α_2 and α_3, are satisfying the compatibility conditions (9), in both cases. Based on these, two main solutions are obtained for the angles φ_{21}^0, φ_{31}^0 and, implicitly, for the angles β_{12}, β_{23} (see Fig. 4,c and d), which assure the homokinetic transmission of motion, , in one of the solutions, the angle β (see Fig. 4, c and d) is noted with a star ($\beta_{12}^*, \beta_{23}^*$).

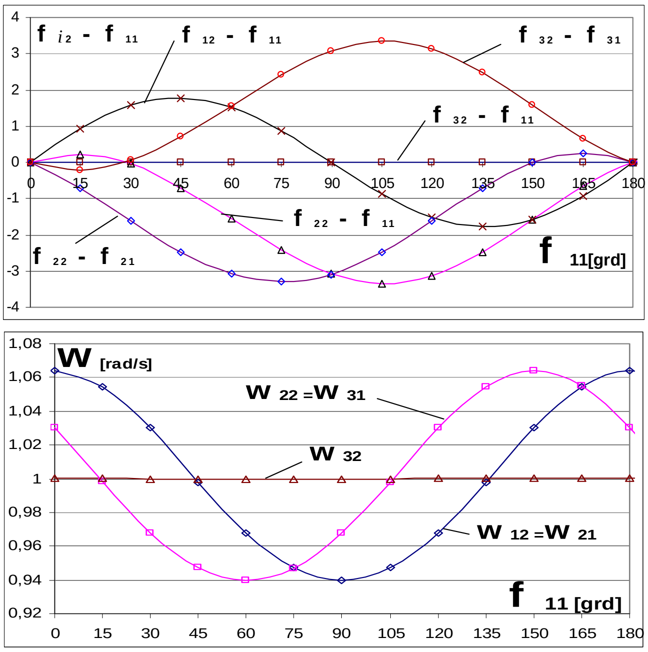

Fig. 5 The variations of angular differences and of angular velocities of cardanic shafts which corresponding to the scheme from fig. 4, a.

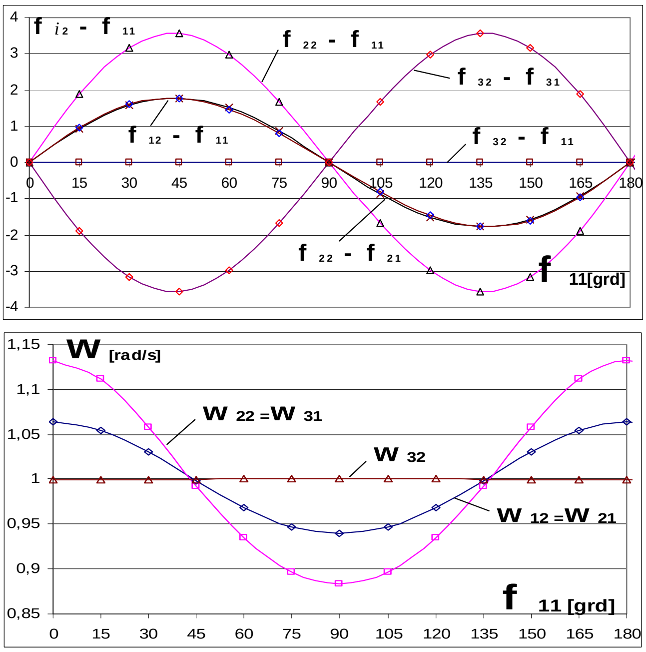

Fig. 6 The variations of angular differences and of angular velocities of cardanic shafts which corresponding to the scheme from fig. 4, b.

In the case of the double solutions (see tab. 1), the designer continue to establish the acceptable variant based on a supplementary criterion.

To show the homokinetics of these transmissions, in Fig. 5 and 6, are presented the variations of the angular differences and angular velocities of Cardan shafts, after numeric simulations; from these graphics result $\varphi_{32} = \varphi_{11}$, and $\omega_{32} = \omega_{11}$ for each value of φ_{11}, which means that these three transmissions are homokinetic.

3. CONCLUSION

Based on cinematic model and on the presented examples, the paper work gives on analysis and synthesis algorithm of n-Cardan mechanisms for which are known the angle δ_{ij} and γ_{ij} (formed by Cardan shafts with the two planes of rectangular projection).

REFERENCES

1. Duditza, F. Kardangelenkgetriebe und ihre Anwendungen, Düsseldorf, VDI–Verlag, 1973
2. Fl. Dudiță, D.V. Diaconescu, M. Neagoe, R. Săulescu. On the modelling of homokinetical tricardanic transmissions. 2nd International Conference „Research and development in mechanical industry" RaDMI 2002, 02 – 04 September, Vrnjacka Banja, Yugoslavia, ISBN 86-83803-03-1, vol II, pp. 872 – 877.
3. Diaconescu, D., Böhm, Ch., Neagoe, M., Jaliu, C. The precision analysis of a classical cardan mechanism on the basis of Different spatial configurations. Bulletin of the Transilvania University of Braşov, vol. 5 (40) - series A, Braşov, pp.37-44, 1998.